Available online at www.sciencedirect.com
ScienceDirect
Journal of the European Ceramic Society 31 (2011) 2513–2518
www.elsevier.com/locate/jeurceramsoc

Processing of a natural hydroxyapatite powder: From powder optimization to porous bodies development

M. Lombardi [a,*], P. Palmero [a], K. Haberko [b], W. Pyda [b], L. Montanaro [a]

[a] Politecnico di Torino, Dept. of Materials Science and Chemical Engineering, INSTM R.U. PoliTO LINCE Lab., C.so Duca degli Abruzzi 24, Torino, Italy
[b] AGH University of Science and Technology, Faculty of Materials Science and Ceramics, A. Mickiewicza 30 Ave., Krakow, Poland

Available online 5 March 2011

Abstract

This paper deals with the development of macro-porous components made of a carbonated hydroxyapatite (HAp) nanopowder which was extracted from pig bones. Prior to sintering, the powder was treated at 700 °C for 1 h. During calcination, a partial carbonate decomposition occurred yielding CaO. In order to eliminate this by-product, the calcined HAp was washed in distilled water several times, checking the effect of washings by FT-IR spectroscopy. Then, the thermal stability of the as-calcined and washed powders treated in the range 800–1400 °C was investigated by XRD.

After that, macro-porous materials made of washed HAp powder were prepared through a modified gelcasting process, using agar as a natural gelling agent and polyethylene spheres as the pore formers.

Keywords: Apatite; Biomedical applications; Calcination; Gelcasting; Porosity

1. Introduction

An ideal scaffold would mimic the matrix of the tissue to be replaced acting as a three-dimensional template. The cells can attach themselves to the template and then grow, migrate and function.[1,2] The scaffold must be made of a biocompatible material (preferably bioactive or resorbable) and must show an interconnected macro-porous network so that cell penetration, tissue ingrowth and vascularisation may occur.[2–6]

The rate and the quality of bone integration are influenced by various microstructural features. These include mean size and total volume of pores, size and amount of interconnections, and walls microstructure. Pores must present size between 100 and 400 μm[3–5] and interconnections of about 50 μm are needed for bone ingrowth.[4] The interconnectivity and the pore volume are necessary for the development of a vascular network for transporting oxygen and nutrients efficiently.[3,4,7] This development must take place before the formation of the new bone. Finally, the walls microstructure, and particularly their micron-sized porosity, can influence the biological response of the scaffold, because of the cell attachment, a possible selective sequestering and binding of adhesion proteins.[4]

Recently hydroxyapatite (HAp, $Ca_{10}(PO_4)_6(OH)_2$) was demonstrated to be an attractive material for biomedical applications since it presents a chemical composition close to that of the bone mineral.[8] In particular, biological apatites contain cationic (i.e. Na^+, Mg^{2+}, K^+, Sr^{2+}, Zn^{2+}, Ba^{2+}, Al^{3+}) or anionic (i.e. F^-, Cl^-, SiO_4^{4-} and CO_3^{2-}) or both of these substitutions.[9] The carbonate ions can occupy the sites of the hydroxyl and the phosphate ions in the apatite structure, giving A- or B-type carbonated hydroxyapatites, respectively. If these substitutions take place simultaneously, an AB-type substitution occurs, as in the case of the bone mineral.[8,10]

One of the simplest ways to produce carbonated HAps is the extraction from natural sources such as fish, bovine or pig bones through thermal, subcritical water or alkaline hydrothermal processes.[11–13]

The organic matter present in these natural sources can be decomposed, dissolved or hydrolysed with these methods,[11] preserving the chemical composition and the structure of the HAp phase.[13] Nevertheless, carbonated HAps present a low thermal stability, since they undergo carbonate loss during thermal treatment required for sintering ceramic parts or coatings.[8,14] The decarbonation yields CaO,[13] which negatively affects the

* Corresponding author at: IIT @ POLITO, Centre for Space Human Robotics, C.so Trento 21, 10129 Torino, Italy. Tel.: +39 011 0903406; fax: +39 011 0903401.
E-mail address: mariangela.lombardi@iit.it (M. Lombardi).

0955-2219/$ – see front matter © 2011 Elsevier Ltd. All rights reserved.
doi:10.1016/j.jeurceramsoc.2011.02.017

biocompatibility[15] and the mechanical response[16] of the sintered materials. However, it was demonstrated that the carbonate loss can be avoided by carrying out thermal treatments in a carbon dioxide atmosphere.[14,17]

In a previous paper a chemical procedure was set up for extracting a natural, carbonated HAp from pig bones.[13] This powder was nonstoichiometric and underwent decarbonation phenomena starting from 700 °C in air atmosphere.

In this paper the aforementioned natural, carbonated HAp was employed for the production of macro-porous components. However, in order to avoid the CaO development during thermal treatment in air, a preliminary calcination at 700 °C for 1 h was performed, thus promoting decarbonation. Subsequently, the powder was washed in distilled water, to exploit the high solubility of $Ca(OH)_2$. The efficiency of the washing process was investigated by Fourier Transform Infrared (FT-IR) Spectroscopy. In addition the thermal stability of the washed powder was investigated by X-Ray Diffraction (XRD) and compared with that of the as-calcined powder.

From the washed HAp, macro-porous components were produced by means of a modified gelcasting procedure.[18] This method exploited agar as the gelling agent and polyethylene spheres as the pore formers. In this way it was possible to control porosity features in terms of shape, size and volume percentage of pores.

2. Materials and methods

2.1. Powder synthesis and characterization

The natural HAp powder was extracted from the cortical part of long pig bones following a procedure deeply described in a previous paper.[13] Clean cortical parts of long pig bones were treated with a hot NaOH water solution for 48 h. In order to remove the remaining sodium hydroxide, the material was carefully washed with distilled water until a pH of 7 was reached in the filtrate. The material was then dried at 120 °C in air atmosphere, ground in an alumina mortar and then calcined at 400 °C for 30 min in order to remove any organic by-products. Only the HAp phase was detected by XRD.

The natural, carbonated HAp presented a specific surface area (SSA, by the Brunauer–Emmett–Teller (BET) N_2 adsorption method) of 72 m^2/g and it was nonstoichiometric, with a Ca/P ratio of 1.72. More details on this powder were already published elsewhere.[13]

The high SSA of this natural HAp implied a low solid loading in aqueous suspension: in fact, very high slurry viscosities were reached starting from 30 mass% HAp. This limited its application through wet forming methods. For this reason, the powder was calcined at 700 °C for 1 h in air (heating and cooling rate of 10 °C/min). This material will be referred to as HA-N.

The natural, carbonated HAp underwent carbonate decomposition during the calcination. To remove CaO prior to sintering, HA-N was washed several times in distilled water, to exploit the high solubility of $Ca(OH)_2$.[17] Washings were repeated until a pH of 7 was reached in the filtrate. The washed powder will be referred to as HA-NW.

HA-N and HA-NW powders were characterized by FT-IR (Bruker FTIR Equinox 55 spectrophotometer equipped with a MCT detector) and XRD (Philips PW 1710 diffractometer). A comparison of the results allowed us to evaluate the efficiency of the washing process.

Infrared spectra were collected in the region 400–4000 cm^{-1}on powders pressed into pellets with KBr. XRD was carried out using Cu Kα radiation (1.541874 Å), in the range 10–55°2θ, with a step size of 0.02°2θ and an acquisition time per step of 2 s, on as-prepared HA-N and HA-NW powders as well as on materials calcined in a wide temperature range (800–1400 °C, 1 h soaking at the maximum temperature, heating and cooling rate of 10 °C/min), to investigate their thermal stability at high temperatures.

The specific surface area of the HA-N and HA-NW powders was measured by the BET N_2 adsorption method (Micromeritics BET model ASAP 2010 M).

To produce dense, as reference materials, and porous components, a modified gelcasting procedure was applied, as previously described in more details.[18]

2.2. Dense bodies elaboration

An aqueous suspension of the HA-NW powder with a solid content of 65 mass% was prepared by using a commercially available dispersant (Duramax D-3021, Rohm and Haas, France, ammonium salt of polycarboxylic acid). The slurry was dispersed under magnetic stirring for 24 h: the agglomerate size distribution as a function of dispersion time was followed by laser granulometry (Fritsch Analysette 22 Compact).

A high purity agar (Sigma–Aldrich, A7049), a polysaccharide constituted by chains of chains of glycosyl units,[19] was used as the gelling agent.

The agar was dissolved in distilled water (2 mass%) at 90 °C, then cooled down to 60 °C and mixed with the dispersed ceramic slurry at the same temperature. The agar content in the ceramic suspension was 0.75 mass% on the basis of the total water amount; the final solid loading of the ceramic slurries was 60 mass%. The obtained suspension was cast into PMMA cylindrical moulds with an internal diameter of 14 mm and a height of 30 mm. In order to remove air bubbles entrapped in the ceramic suspension, cast was carried out under vacuum (at about 10^{-2} Pa).[20] Gelation occurred during cooling down to room temperature. The gelled pieces were de-moulded after 24 h and dried in controlled humidity conditions. During drying, gelcast components underwent a shrinkage of about 30 vol%.

These samples will be referred to as no-PE materials.

2.3. Porous bodies elaboration

For the development of macro-porous samples, polyethylene spheres (PE, supplied by Clariant Italia SpA; density of about 0.93 g/cm^3) were used as a fugitive phase, as described elsewhere.[18] The PE powder was sieved, selecting two fractions as pore formers: the former made of smaller spheres with diameters between 224 and 355 μm (referred to as SS), the latter made of larger spheres in the range 355–425 μm (referred to as LS).

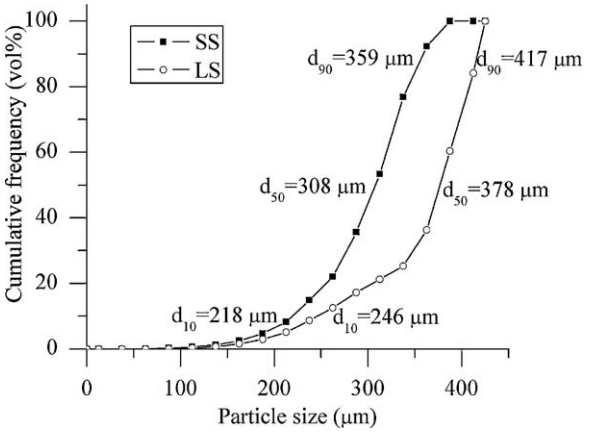

Fig. 1. Particle size distribution of the PE fractions.

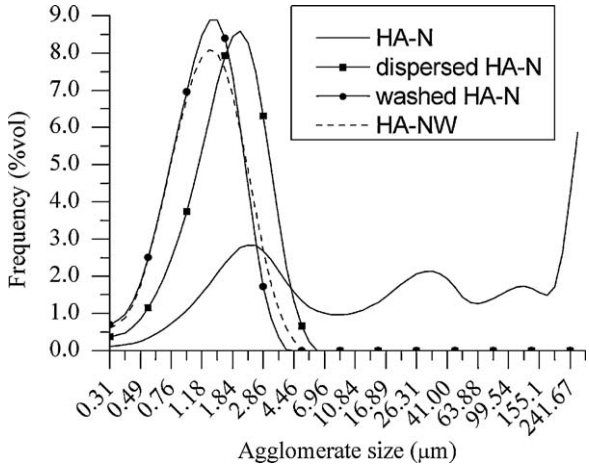

Fig. 2. Agglomerate size distribution of the HA-N and HA-NW powders.

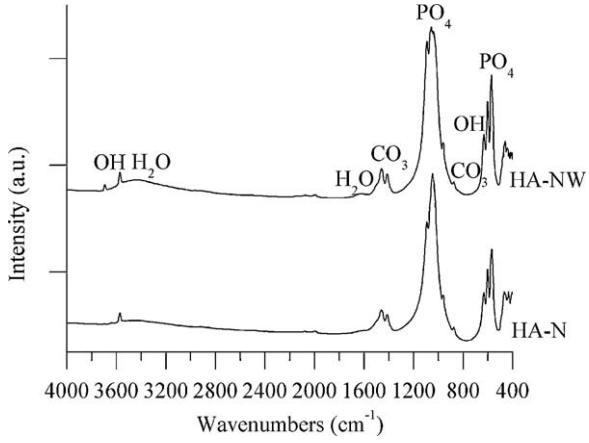

Fig. 3. FT-IR spectra of the HA-N and HA-NW powders.

Their size distributions, estimated by image analyses performed on several Scanning Electron Microscope (SEM, Hitachi S2300) micrographs, are shown in Fig. 1. Various PE spheres smaller than the lower sieving limit were observed. Their presence is probably due to their electrostatic adhesion to the surface of other PE spheres during sieving.

The PE spheres were mixed in the dispersed HAp suspension in a fixed amount to reach a porosity of 60 vol% in the fired materials. After that, the slurry was homogenized for 1 h under magnetic stirring and finally the agar was added before casting, as previously described. These samples will be referred to as PE materials.

The gelcast green bodies were sintered at 1300 °C for 3 h (heating rate of 2 °C/min). In the case of porous materials, several heating and isothermal steps below 600 °C were performed during the thermal cycle, to obtain the thermal decomposition of the PE spheres[18] without affecting the integrity of the green bodies. Green and fired densities of the gelcast components were evaluated by weight and geometrical measurements. The fired components were characterized by SEM and Hg porosimetry (Carlo Erba Porosimeter 2000), to evaluate microstructural features, pore size distribution and open porosity percentage.

3. Results and discussion

After calcination at 700 °C for 1 h, HA-N presented a SSA of 1.4 m^2/g. A relevant agglomeration was induced by the thermal treatment, as shown by the agglomerate size distribution reported in Fig. 2. In spite of this, the powder was dispersed in distilled water under magnetic stirring after 10 h. The resultant suspension was characterized by a very high pH value (14.0), due to CaO dissolution as calcium hydroxide in water.

The agglomerates of the HA-N powder were partially dispersed during washings and the subsequent drying step to produce HA-NW did not imply re-agglomeration (Fig. 2).

Moreover, the washings also implied a slight SSA increase (3.1 m^2/g) and a decrease of the pH suspension to 9.

The FT-IR spectra of the two powders (Fig. 3) showed the characteristic bands of the carbonated HAps: signals related to the vibrations of P–O bonds[8,13] were recorded in the range 471–603 and 992–1091 cm^{-1}. The bands at 630 and 3570 cm^{-1} were assigned to the apatitic OH groups.[21] The HA-NW powder also presented two broad bands in the regions 1600–1700 and 3200–3700 cm^{-1} corresponded to the adsorbed water.[8,10]

As concerns the carbonate vibrations, generally they were recorded in two ranges, 850–890 cm^{-1} and 1400–1650 cm^{-1}; an enlargement of these regions (Fig. 4) proved that the two HAps were B-types carbonated.[8] This feature could explain the nonstoichiometry of the starting natural hydroxypatite.[13]

From the above results, it is reasonable to suppose that the washing process does not change the structure of the natural powder, but implies a surface modification and the water adsorption.

A different thermal stability was observed for these powders. HA-N underwent decomposition phenomena yielding small amounts of CaO from 800 °C (Fig. 5a) and $NaCaPO_4$ from 1100 °C (Fig. 5b), as already observed for the natural hydroxyapatite.[17] In fact, it has been demonstrated that these compounds can be yielded by high-temperature reactions between HAp and Na ions.[22]

In the case of HA-NW traces of CaO appeared (Fig. 5c) only after calcination at 1300 °C. The increase in thermal stability

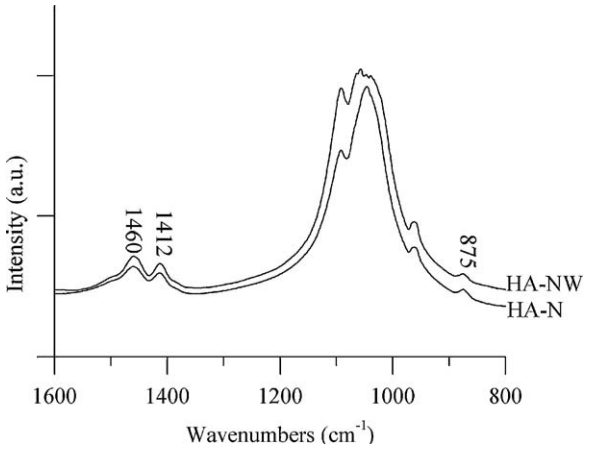

Fig. 4. Carbonates bands of the HA-N and HA-NW powders.

after the washing processes could be attributed to the removal of Na ions, derived by the extraction treatment.

These results indicated that the HA-N powder underwent decomposition phenomena induced by the presence of residual Na ions, without decarbonation. Washing was able to improve the thermal stability of the carbonated HAp removing sodium ions as well as CaO developed during the thermal treatment of the powder.

A slightly higher dispersability of the HA-NW powder was reached by adding a dispersant (Duramax D-3021), as reported in Table 1. In addition, higher solid contents, suitable for the improvement of the green density,[23] were reached.

Gelcast no-PE HA-NW samples presented a mean green density of 1.55 g/cm^3, corresponding to 49%TD (theoretical density of 3.16 g/cm^3). After sintering at 1300 °C for 3 h, a mean density of 2.56 g/cm^3 (81%TD) was reached. This is due to an incomplete HAp densification, as shown in the Fig. 6. These components were characterized by a micron-sized grain size and a residual porosity of about 1 μm in radius, as confirmed by the Hg porosimetry.

Table 1
d_{10}, d_{50} and d_{90} values of the dispersed HA-NW powder with and without dispersant.

	d_{10}	d_{50}	d_{90}
Dispersed HA-NW without dispersant	0.71	1.68	4.13
Dispersed HA-NW with dispersant	0.63	1.46	3.24

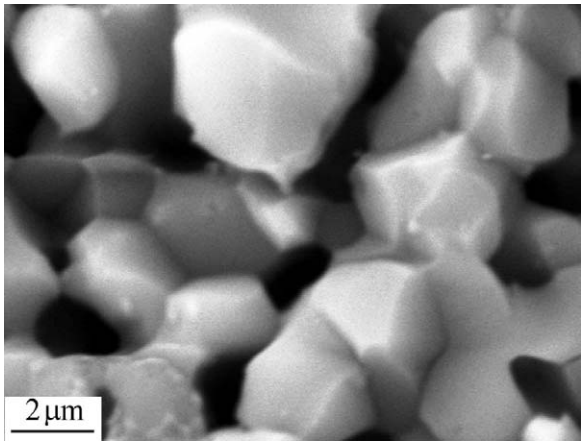

Fig. 6. SEM image of the fracture surface of a no-PE HA-NW sample.

A total pore volume of 20% was determined for the no-PE HA-NW samples. The pores were almost completely open as also confirmed by the density data.

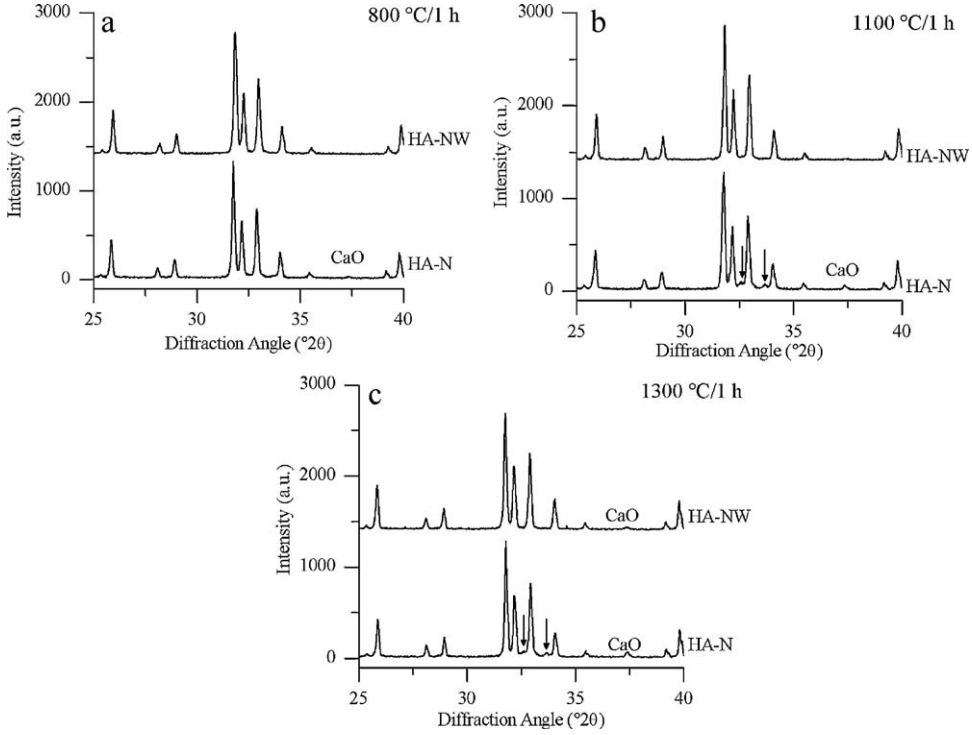

Fig. 5. XRD of the calcined HA-N and HA-NW powders (peaks without marks are indexed as HAp phase, arrows indicated $NaCaPO_4$ peaks).

Table 2
Density values of the macro-porous materials.

	HA-NW_LS	HA-NW_SS
Green density (g/cm^3)	1.08 [60%TD*]	1.05 [58%TD*]
Fired density (g/cm^3)	1.28 [40%TD]	1.30 [41%TD]

As concerns the PE cast pieces, two PE fractions were exploited for producing two types of porous materials, named HA-NW_LS and HA-NW_SS. Their green and fired densities are listed in Table 2. A theoretical density of 1.82 g/cm^3 was calculated using the rule of the mixture in the case of green components.

The fired PE components were characterized by a homogeneous distribution of the macro-pores generated by the pore former decomposition, as illustrated in Fig. 7. Some cracks were induced during sample polishing performed to obtain flat surfaces for image analyses.

The apparent macro-pore size distribution (Fig. 8) was in fact evaluated by image analyses performed on these 2D sections; as a consequence, the pore data are related, but not equivalent, to the real diameters in a 3D space.

Obviously, the particle size distribution of the pore formers and the shrinkage during sintering determined the pore diameters in fired components. Moreover, the porosimetric analyses

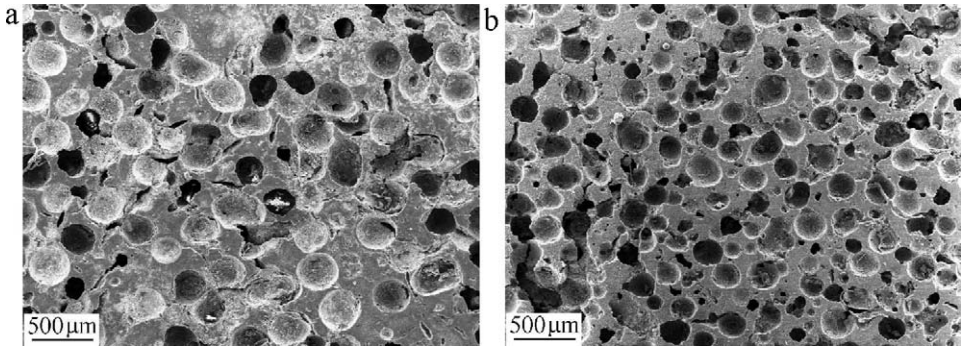

Fig. 7. SEM images of the polished surfaces of (a) HA-NW_LS and (b) HA-NW_SS samples.

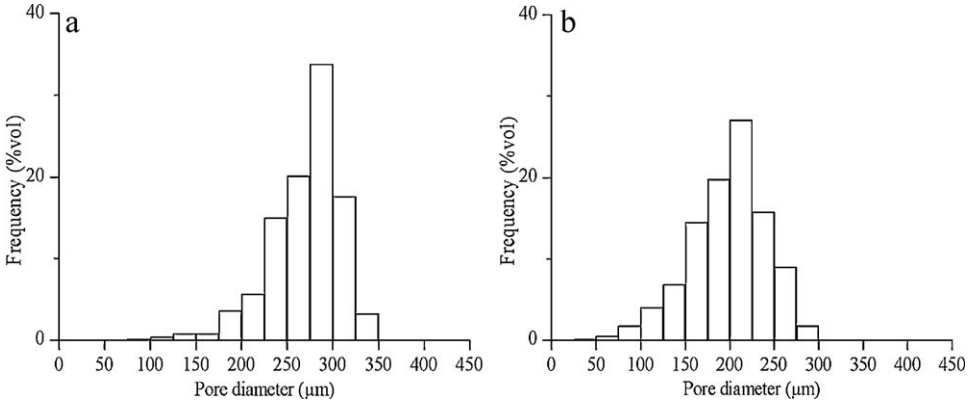

Fig. 8. Apparent pore size distribution of (a) HA-NW_LS and (b) HA-NW_SS samples by image analyses.

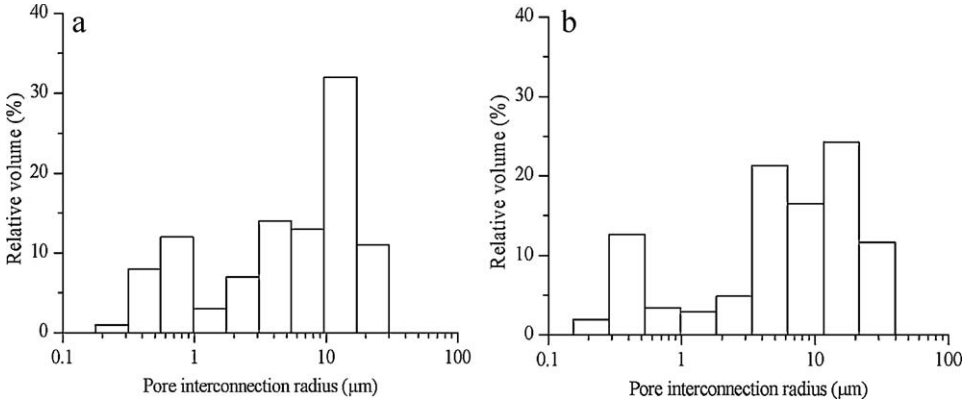

Fig. 9. Pore interconnection radius distribution of (a) HA-NW_LS and (b) HA-NW_SS samples.

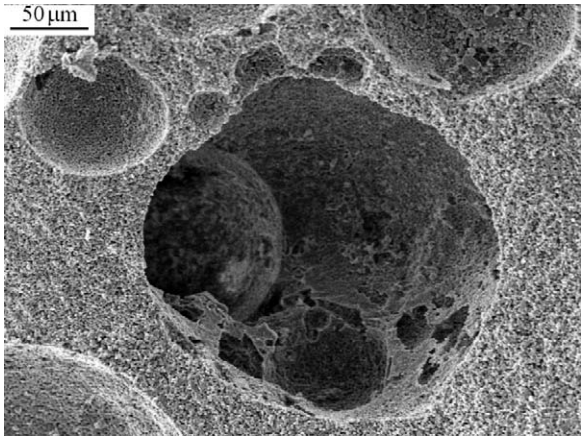

Fig. 10. SEM micrograph showing a detail of a porous component: interconnectivity among pores.

(Fig. 9) showed that the sizes of the PE spheres also affect the interconnection features.

In fact, all the components presented a bimodal distribution: the lower classes (below about 1 μm) can be imputed to the access of micron-sized pores on the ceramic walls (similarly to those observed for the no-PE samples), whereas the bigger ones are due to the interconnections among the macro-pores (see for instance Fig. 10).

An apparent density value of about 1.5 g/cm^3 (corresponding to 48%TD) was determined for all PE materials, independently from the PE fraction. In contrast, the pore former size affects the total open porosity: in fact, values of 42 and 51 vol% were measured for LS and SS materials, respectively. On the ground of these results, it can be reasonably supposed that the finer PE fraction implied the development of a more interconnected porosity. This can be explained considering that in a volume unit the smaller the spheres, the higher the number of contact points.

4. Conclusions

A washing procedure was set up for avoiding the thermal decomposition of a natural carbonated hydroxyapatite. The washed powder was made of dispersed, micron-sized particles of a B-type carbonated hydroxyapatite phase, thermally stable up to 1300 °C. This powder presented a lower SSA and a modified surface with respect to the starting hydroxyapatite. As a consequence, the aqueous suspension of this powder presented a better dispersability and a pH value more appropriate to gelcasting.

Porous components having controlled porosity features, such as mean size and total volume of pores, size and amount of interconnections, and walls microstructure, were produced through a modified gelcasting method.

Acknowledgements

The authors wish to thank the European Commission for partially supporting this work in the framework of the Integrated Project "NANOKER–Structural Ceramic Nanocomposites for top-end Functional Applications", contract n°: NMP3-CT-2005-515784 (www.nanoker-society.org).

References

1. Freyman TM, Yannas IV, Gibson LJ. Cellular materials as porous scaffolds for tissue engineering. *Prog Mater Sci* 2001;**46**:273–82.
2. Jones JR, Hench LL. Regeneration of trabecular bone using porous ceramics. *Curr Opin Solid State Mater Sci* 2003;**7**:301–7.
3. Barrère F, Mahmood TA, de Groot K, van Blitterswijk CA. Advanced biomaterials for skeletal tissue regeneration: instructive and smart functions. *Mater Sci Eng R* 2008;**59**:38–71.
4. Hing KA. Bioceramic bone graft substitutes: influence of porosity and chemistry. *Int J Appl Ceram Tech* 2005;**2**:184–99.
5. Hutmacher DW, Schantz JT, Lam CXF, Tan KC, Lim TC. State of the art and future directions of scaffold-based bone engineering from a biomaterials perspective. *J Tissue Eng Regen Med* 2007;**1**:245–60.
6. Will J, Melcher R, Treul C, Travitzky N, Kneser U, Polykandriotis E, et al. Porous ceramic bone scaffolds for vascularized bone tissue regeneration. *J Mater Sci: Mater Med* 2008;**19**:278–90.
7. Best SM, Porter AE, Thian ES, Huang J. Bioceramics: past, present and for the future. *J Eur Ceram Soc* 2008;**28**:1319–27.
8. Lafon JP, Champion E, Bernache-Assollant D. Processing of AB-type carbonated hydroxyapatite $Ca_{10-x}(PO_4)_{6-x}(CO_3)_x(OH)_{2-x-2y}(CO_3)_y$ ceramics with controlled composition. *J Eur Ceram Soc* 2008;**28**:139–47.
9. Elliott J. *Structure and chemistry of the apatites and other calcium orthophosphates*, vol. 74. Amsterdam: Elsevier Science; 1994.
10. Barinov SM, Fadeeva IV, Ferro D, Rau JV, Cesaro SN, Komlev VS, et al. Stabilization of carbonate hydroxyapatite by isomorphic substitutions of sodium for calcium. *Russ J Inorg Chem* 2008;**53**:164–8.
11. Barakat NAM, Khil MS, Omran AM, Sheikh FA, Kim HY. Extraction of pure natural hydroxyapatite from the bovine bones bio waste by three different methods. *J Mater Process Technol* 2009;**209**:3408–15.
12. Barakat NAM, Khalil KA, Sheikh FA, Omran AM, Gaihre B, Khil SM, et al. Physiochemical characterizations of hydroxyapatite extracted from bovine bones by three different methods: extraction of biologically desirable HAp. *Mater Sci Eng C* 2008;**28**:1381–7.
13. Haberko K, Bucko MM, Brzezinska-Miecznik J, Haberko M, Mozgawa W, Panz T, et al. Natural hydroxyapatite – its behaviour during heat treatment. *J Eur Ceram Soc* 2006;**26**:537–42.
14. Barinov SM, Rau JV, Cesaro SN, Durišin J, Fadeeva IV, Ferro D, et al. Carbonate release from carbonated hydroxyapatite in the wide temperature rage. *J Mater Sci: Mater Med* 2006;**17**:597–604.
15. Joschek S, Nies B, Krotz R, Göpferich A. Chemical and physicochemical characterization of porous hydroxyapatite ceramics made of natural bone. *Biomaterials* 2000;**21**:1645–58.
16. Slosarczyk A, Stobierska E, Paszkiewicz Z, Gawlicki M. Calcium phosphate materials prepared from precipitates with various calcium:phosphorus molar ratios. *J Am Ceram Soc* 1996;**79**:2539–44.
17. Haberko K, Bucko MM, Mozgawa W, Pyda A, Brzezinska-Miecznik J, Carpentier J. Behaviour of bone origin hydroxyapatite at elevated temperatures and in O_2 and CO_2 atmospheres. *Ceram Int* 2009;**35**:2537–40.
18. Lombardi M, Naglieri V, Tulliani J-M, Montanaro L. Gelcasting of dense and porous ceramics by using a natural gelatine. *J Porous Mater* 2009;**16**:393–400.
19. Olhero SM, Tarì G, Coimbra MA, Ferreira JMF. Synergy of polysaccharide mixtures in gelcasting of alumina. *J Eur Ceram Soc* 2000;**20**:423–9.
20. Omatete OO, Janney MA, Strehlow RA. Gelcasting – a new ceramic forming process. *Ceram Bull* 1991;**70**:1641–9.
21. Lafon JP, Champion E, Bernache-Assollant D, Gibert R, Danna AM. Thermal decomposition of carbonated calcium phosphate apatites. *J Therm Anal Calorim* 2003;**72**:1127–34.
22. Jalota S, Bhaduri SB, Tas AC. A new Rhenanite (β-$NaCaPO_4$) and hydroxyapatite biphasic biomaterial for skeletal repair. *J Biomed Mater Res B* 2007;**80**:304–16.
23. Lewis JA. Colloidal processing of ceramics. *J Am Ceram Soc* 2000;**83**:2341–59.